

A Novel Cytochrome P450, Zebrafish Cyp26D1, Is Involved in Metabolism of All-*trans* Retinoic Acid

Xingxing Gu,* Fang Xu,* Wei Song, Xiaolin Wang, Ping Hu, Yumin Yang, Xiang Gao, and Qingshun Zhao

Model Animal Research Center and State Key Laboratory of Pharmaceutical Biotechnology (X.Gu, F.X., W.S., X.W., P.H., X.Ga., Q.Z.), Nanjing University, Nanjing 210093, China; Jiangsu Province Key Laboratory of Neuroregeneration (X.Gu, Y.Y.), Nantong University, Nantong 226001, China; and School of Life Sciences (W.S., X.W.), Nanjing Normal University, Nanjing 210097, China

Retinoid signaling is essential for development of vertebrate embryos, and its action is mainly through retinoic acid (RA) binding to its RA receptors and retinoid-X receptors, while the critical concentration and localization of RA in embryos are determined by the presence and activity of retinal dehydrogenases (for RA synthesis) and cytochrome P450 RAs (Cyp26s) (for degradation of RA). Previously, we identified a novel *cyp26* gene (*cyp26d1*) in zebrafish that is expressed in hind-brain during early development. Using reverse-phase HPLC analyses, we show here that zebrafish Cyp26D1 expressed in 293T cells could metabolize all-*trans* RA, 9-*cis* RA, and 13-*cis* RA, but could not metabolize retinol or retinal. The metabolites of all-*trans* RA produced by Cyp26D1 were the same as that produced by Cyp26A1, which are mainly

4-hydroxy-all-*trans*-RA and 4-oxo-all-*trans*-RA. Performing mRNA microinjection into zebrafish embryos, we demonstrated that overexpression of Cyp26D1 in embryos not only caused the distance between rhombomere 5 and the first somite of the injected embryos to be shorter than control embryos but also resulted in left-right asymmetry of somitogenesis in the injected embryos. These alterations were similar to those caused by the overexpression of *cyp26a1* in zebrafish embryos and to that which resulted from treating embryos with 1 μ M 4-diethylamino-benzaldehyde (retinal dehydrogenase inhibitor), implying that *cyp26d1* can antagonize RA activity *in vivo*. Together, our *in vitro* and *in vivo* results provided direct evidence that zebrafish Cyp26D1 is involved in RA metabolism. (*Molecular Endocrinology* 20: 1661-1672, 2006)

RETINOID SIGNALING HAS long been recognized to be crucial to embryonic development. It was first found in the 1930s that farm animals fed with a vitamin A-deficient diet produced abnormal embryos with widespread defects in the eye, craniofacial, limb, heart, and urogenital systems (1). On the other hand, overexposure of retinoid signaling to embryos also disrupted the development of embryos (2). It is known that retinoid signaling is transduced through the ligand, retinoic acid (RA), binding to the heterodimers of RA receptors (RARs) and retinoid-X receptors to regulate expression of target genes containing RA response elements (3). However, gene knockout studies in mice have shown that RARs and retinoid-X receptors can function in a partly redundant manner during development (4). Therefore, the temporal and spatial

regulation of RA presence plays determining roles in retinoid signaling.

RA cannot be synthesized *de novo* in vertebrates. Animals take dietary vitamin A and convert it into RA *in vivo* through two dehydrogenation steps, in which the absorbed vitamin A is first converted into all-*trans* retinaldehyde by retinol dehydrogenase, and retinaldehyde is then oxidized into all-*trans* RA by the retinal dehydrogenase (Raldh) (5). On the other hand, specific cytochrome P450 RAs (Cyp26s) degrade RA into inactive polar forms, such as 4-hydroxy-all-*trans*-RA (4-OH-RA), 4-oxo-all-*trans*-RA (4-oxo-RA), and 18-hydroxy-all-*trans*-RA (18-OH-RA) (5, 6). Because the reaction catalyzed by retinol dehydrogenase is reversible, RA homeostasis is maintained by regulation of its rate of synthesis from retinal and by control of its rate of degradation through oxidative pathways (5).

Three Raldhs (Raldh1, Raldh2, and Raldh3) have been identified in vertebrates. Although genetic ablation of *Raldh1* had no apparent effects on mouse embryo development (7), the phenotypes of mouse embryos with *Raldh2* or *Raldh3* gene disrupted were similar to those observed in vitamin A-deficient fetuses. *Raldh2*-null mice died at midgestation with a shorter anterior-posterior axis, open neural tube, absence of limb buds (8), and asymmetric somitogenesis (9, 10). Similarly, zebrafish *raldh2* mutants (*nls*, *nof*)

First Published Online February 2, 2006

* X.Gu and F.X. contributed equally to this work.

Abbreviations: Cyp26, Cytochrome P450 retinoic acid; DEAB, 4-diethylamino-benzaldehyde; 5,6-epoxy-RA, 5,6-epoxy-all-*trans*-retinoic acid; 4-OH-RA, 4-hydroxy-all-*trans*-retinoic acid; 18-OH-RA, 18-hydroxy-all-*trans*-retinoic acid; 4-oxo-RA, 4-oxo-all-*trans*-retinoic acid; r5, rhombomere 5; RA, retinoic acid; Raldh, retinal dehydrogenase; RAR, retinoic acid receptor; s1, somite 1.

Molecular Endocrinology is published monthly by The Endocrine Society (<http://www.endo-society.org>), the foremost professional society serving the endocrine community.

were characterized with a truncation of the anterior-posterior axis anteriorly to the somites, absence of pectoral fins (11, 12), and asymmetric somitogenesis (13). *Raldh3* knockout in mice caused malformations in ocular and nasal regions, notably resulting in choanal atresia, which is responsible for respiratory distress and death of *Raldh3*-null mutants at birth (14).

Three Cyp26s (Cyp26A1, Cyp26B1, and Cyp26C1) have been characterized in vertebrates (15–22). Although loss of function of *Cyp26C1* during vertebrate development has not been characterized yet, loss of *Cyp26A1* function caused mouse embryonic lethality (23, 24), whereas the *Cyp26B1*-null mouse died after birth (25). *Cyp26A1*-null embryos died from caudal regression associated with exencephaly, spina bifida, agenesis of the caudal portions of the digestive and urogenital tracts, malformed lumbosacral skeletal elements, and lack of caudal tail vertebrae (23, 24). In zebrafish, embryos with *cyp26a1* mutation, *giraffe*, displayed a phenotype just opposite to that of the *raldh2* mutant, exhibiting expanded rostral spinal cord territory (26). Additionally, when *Cyp26A1*^{-/-} homozygous mice were bred into a *Raldh2*^{+/-} background, the *Cyp26A1*-null phenotypes were suppressed, suggesting that a function of Cyp26A1 could be to titrate the local level of RA to prevent inappropriate RA signaling (6). *Cyp26B1*^{-/-} mice manifested various malformations, including meromelia, micrognathia, and open eyes at birth, and they died immediately after birth as a result of respiratory distress (25).

Previously, we described a novel *cyp26*, *cyp26d1*, in zebrafish (27). Here, we provide *in vitro* and *in vivo*

evidence to demonstrate that, like other Cyp26 members, zebrafish *cyp26d1* is involved in the metabolism of RA.

RESULTS

Zebrafish Cyp26D1 Contains the Conserved Functional Domains Found in Other Cyp26s

Previously, we had cloned a novel *cyp26* (*cyp26d1*) in zebrafish (27). Bioinformatic analysis suggested that *cyp26d1* defines a new Cyp26 subfamily rather than being an ortholog of any known mammalian Cyp26 member (27). By comparing its predicted amino acid sequence to mouse Cyp26A1 and zebrafish Cyp26A1, we found that the predicted functional domains in Cyp26, including anchor domain, proline domain, oxygen binding domain, retinoid domain, and heme-binding domain are all conserved in Cyp26D1 (28) (Fig. 1). The sequence characteristics of Cyp26D1 suggest that it would be involved in the metabolism of RA.

Zebrafish Cyp26D1 Specifically Metabolizes RA, But Not Retinol or Retinal

To examine whether zebrafish Cyp26D1 can metabolize RA, we first overexpressed *cyp26d1* in 293T cells. Because Cyp26D1 possesses a transmembrane domain typical of microsomal-associated P450s (anchor region; Fig. 1), microsomal fractions of the cells overexpressing Cyp26D1 were collected and then incu-

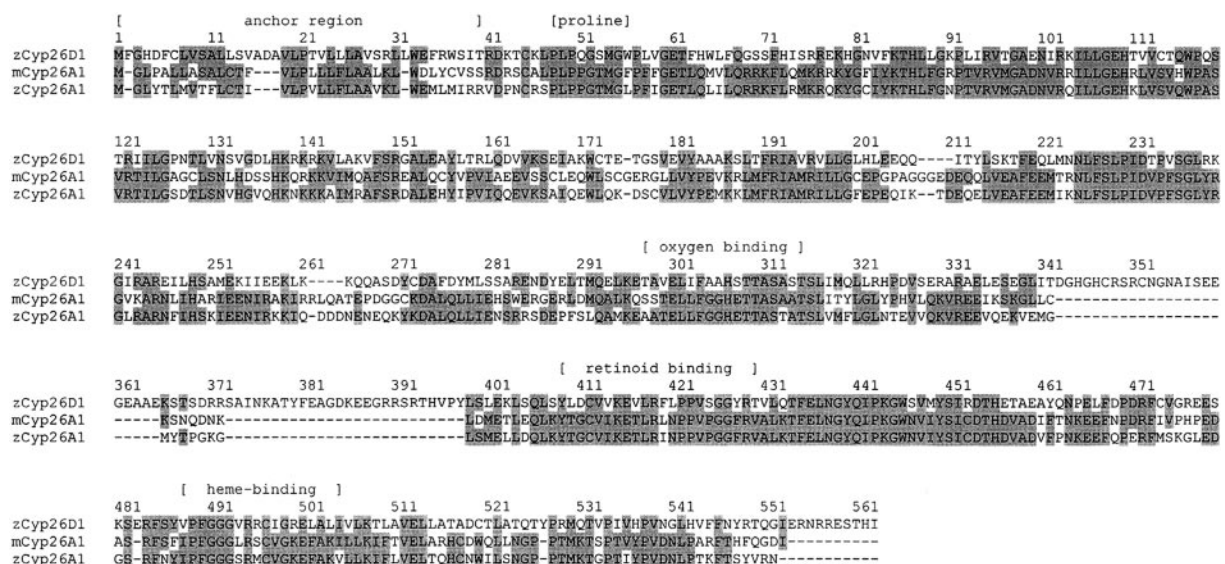


Fig. 1. Sequence Alignment of Zebrafish Cyp26D1 with Mouse Cyp26A1 and Zebrafish Cyp26A1

The amino acid identities of zebrafish Cyp26D1 (AY920470) with mouse Cyp26A1 (NP_031837) and zebrafish Cyp26A1 (U68234) were determined using Jellyfish software (www.biowire.com; version 1.4). Identical amino acid residues are cross-hatched, and dashes represent gaps for alignment purposes. The predicted conserved functional domains in CYPs, as described in previous work (28), are indicated by bracketing above the Cyp26 sequences. Anchor region, Predicted membrane-spanning helix; proline, proline-rich domain; oxygen binding, sites of oxygen binding; retinoid binding, predicted retinoid binding region; heme-binding, consensus sequence for the heme-binding pocket; z, zebrafish; m, mouse.

bated with various retinoids to allow the expressed Cyp26D1 to metabolize retinoids. After reaction, the retinoids and their metabolites from the reaction mixtures were extracted and then analyzed by reverse-phase HPLC. As shown in Fig. 2B, in addition to a peak corresponding to unmetabolized all-*trans* RA (Table 1), two major peaks along with two small peaks were displayed after the retinoid was incubated with microsomes of *cyp26d1*-expressing cells. In contrast, extraction of the reaction mixture incubated with microsomes of cells transfected with vehicle vector only yielded one peak that corresponded to the unmetabolized all-*trans* RA (Fig. 2A and Table 1), indicating that microsomes from 293T cells themselves do not have detectable activity to metabolize all-*trans* RA. Therefore, our results revealed that zebrafish Cyp26D1 could metabolize all-*trans* RA into at least four different metabolites. When 9-*cis* RA was used as a substrate, extraction of the reaction mixture incubated with microsomes of *cyp26d1*-expressing cells exhibited one extra major peak along with one small peak (Fig. 2D), in addition to the peak corresponding to unmetabolized 9-*cis* RA (Fig. 2D and Table 1). When 13-*cis* RA was used as a substrate, in addition to the peak of unmetabolized 13-*cis* RA (Fig. 2F and Table 1), extraction of the reaction mixture after incubation with microsomes from *cyp26d1*-expressing cells produced two additional major peaks (Fig. 2F). In contrast, extraction of the reaction mixture of 9-*cis* RA and 13-*cis* RA incubated with microsomes of cells transfected with vehicle vector only yielded one peak that corresponded to the unmetabolized 9-*cis* RA and 13-*cis* RA, respectively (Fig. 2, C and E, and Table 1), indicating that microsomes from 293T cells themselves do not have detectable activity to metabolize 9-*cis* RA or 13-*cis* RA. Furthermore, when retinol or all-*trans* retinal were used as substrates, extraction of reaction mixtures gave only one peak (Fig. 2, G and H) that corresponded to the unmetabolized retinol or all-*trans* retinal, respectively (Table 1), indicating that Cyp26D1 could not metabolize retinol or retinal. Together, these results indicated that Cyp26D1 could metabolize RA including all-*trans* RA, 9-*cis* RA and 13-*cis* RA, but not retinol or all-*trans* retinal.

The Major Metabolites of All-*trans* RA Produced by Zebrafish Cyp26D1 Include 4-oxo-RA and 4-OH-RA

As shown in Fig. 2B, there were at least four different metabolites (peak 1 and peak 2, p3 and p4, as shown in Fig. 3A) of all-*trans* RA produced by Cyp26D1. To identify them, we compared the metabolites produced by Cyp26D1 with those produced by zebrafish Cyp26A1, because the major metabolites of all-*trans* RA produced by Cyp26A1 had been previously identified as 4-oxo-RA and 4-OH-RA (15). To perform this assay, we added all-*trans* RA as a substrate to react with microsomes isolated from 293T cells expressing zebrafish *cyp26a1* and performed reverse-phase

HPLC with Hypersil BDS C18 column on the reaction mixture. In addition to the peak corresponding to unmetabolized all-*trans* RA, the HPLC analysis also yielded two major peaks (peak 1 and peak 2) along with two small peaks (p3 and p4), which were the same as that exhibited by the *cyp26d1* metabolites (Fig. 3, A and B). Most interestingly, the retention time of each peak from the metabolites produced by Cyp26A1 was similar to those produced by Cyp26D1 (Table 2 and Fig. 3, A and B). We then mixed the extracts from Cyp26D1 reaction mixture with those from Cyp26A1 reaction mixture and performed HPLC analyses using the same column and the same elution conditions and found that all of the peaks including the four different metabolites' peaks and unmetabolized substrate peak were comigrating, respectively (Fig. 3C). This result is consistent with the conclusion that the metabolites produced by zebrafish Cyp26D1 are the same as those produced by zebrafish Cyp26A1. To further confirm this, we performed reverse-phase HPLC on the metabolites with a different type of column (SB-phenyl column), using a different eluting condition. And that produced the same result. As with the C18 column, HPLC analyses using the SB-phenyl column on reaction mixture metabolized by Cyp26D1 or Cyp26A1 both exhibited two major peaks along with two small peaks, respectively, in addition to one peak of unmetabolized all-*trans* RA (Fig. 3, D and E, and Table 2). Also, the four peaks from Cyp26D1 reaction and Cyp26A1 reaction have similar retention times (Fig. 3, D and E, and Table 2). When two sources of the metabolites were mixed together to run the SB-phenyl column, all five peaks including the four metabolites' peaks and one unmetabolized all-*trans* RA peaks were comigrating, respectively (Fig. 3F), further proving that the metabolites produced by Cyp26D1 are the same as the metabolites produced by Cyp26A1. Because the major metabolites of all-*trans* RA produced by zebrafish *cyp26a1* were previously identified as 4-oxo-RA and 4-OH-RA (15), therefore our results indicate that like Cyp26A1, the major metabolites of all-*trans* RA produced by Cyp26D1 could also be 4-oxo-RA and 4-OH-RA. When 9-*cis*-RA or 13-*cis*-RA was used as a substrate, our results showed that the peaks of metabolites produced by Cyp26D1 were also comigrating with those produced by Cyp26A1, respectively (Table 2 and data not shown). Together, these results demonstrated that the metabolites of RA produced by Cyp26D1 are the same as that produced by Cyp26A1.

Cyp26D1 Can Inactivate RA *in Vivo*

It has been reported that the distance between rhombomere 5 (r5) and first somite (s1) in *raldh2* mutant (*nls*) embryos is much shorter than that of wild-type zebrafish embryos (11). Because *raldh2* is the major source for RA synthesis, it would be predicted that the distance between r5 and s1 would be shorter if embryos have reduced endogenous RA activity. To ex-

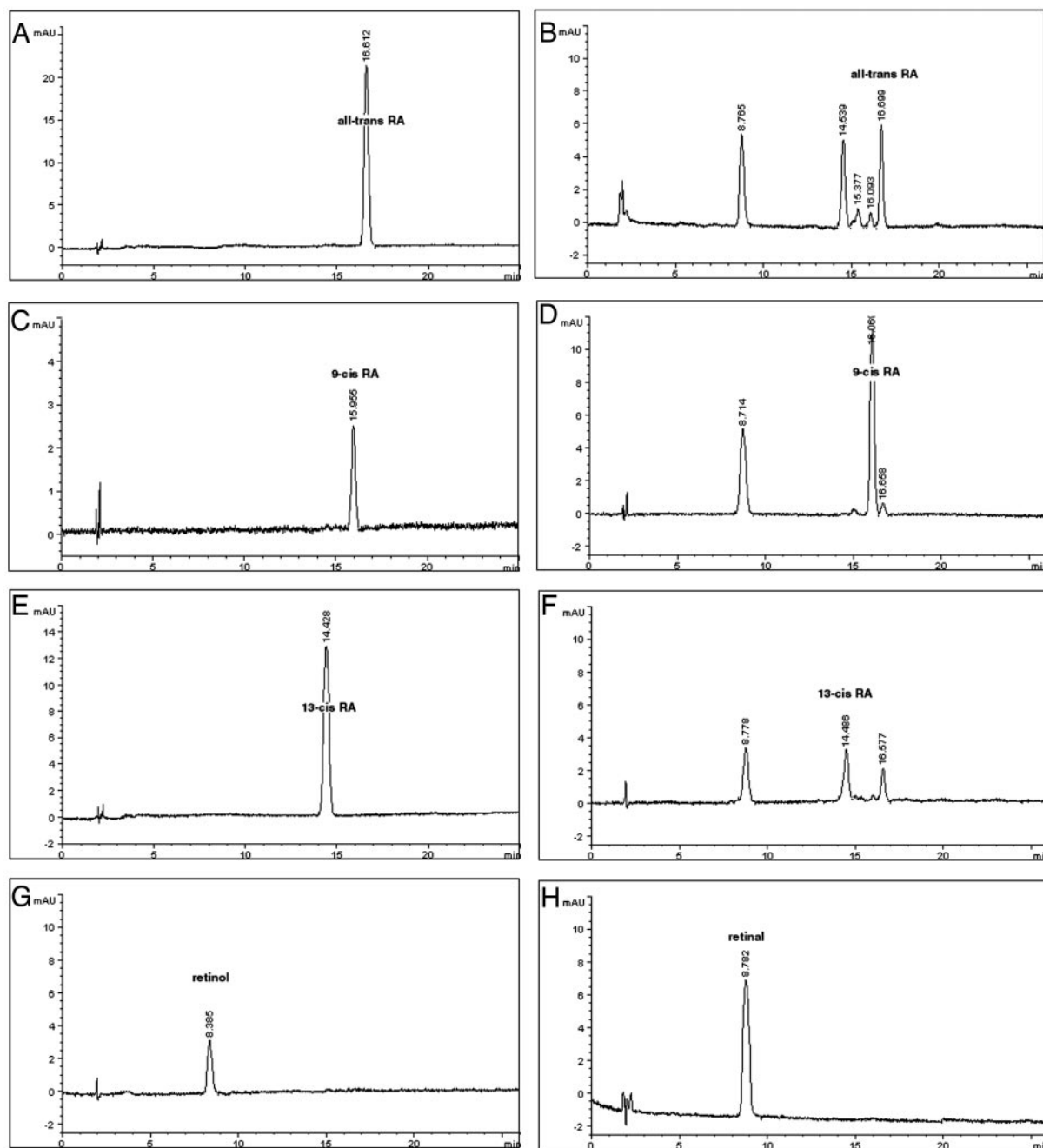


Fig. 2. HPLC Analysis Showing that Zebrafish Cyp26D1 Can Metabolize RA Including All-trans-RA, 9-cis-RA, and 13-cis-RA

All-trans-RA (A and B), 9-cis-RA (C and D), 13-cis-RA (E and F), retinol (G), and all-trans retinal (H) were added as substrates to react with microsomes isolated from 293T cells transfected with vehicle vector or zebrafish *cyp26d1*, respectively. By performing reverse-phase HPLC with a Hypersil BDS C18 column, retinoids extracted from the reaction mixture of all-trans RA, 9-cis-RA, and 13-cis-RA incubated with microsomes of cells transfected with zebrafish *cyp26d1* were separated into two major peaks plus two small peaks (B), one major peak plus a small peak (D), and two major peaks (F), respectively. In contrast, extraction of the reaction mixture of all-trans RA, 9-cis-RA, and 13-cis-RA incubated with microsomes of cells transfected with vehicle vector only yielded one peak that corresponded to the unmetabolized all-trans RA, 9-cis-RA, and 13-cis-RA, respectively (A, C, and E). Furthermore, no metabolite was detected from the reaction mixtures when retinol (G) or all-trans retinal (H) was used as a substrate. Unmetabolized substrates were marked as judged by the retention time of standard all-trans RA, 9-cis-RA, 13-cis-RA, retinol, and all-trans retinal (Table 1). x-axis, Retention time (in minutes) of retinoids; y-axis, absorbance value at 350 nm (mAU).

amine this hypothesis, we treated embryos with 1 μ M 4-diethylamino-benzaldehyde (DEAB) (Raldh inhibitor) until the 11-somite stage (11S). As expected, whole-

mount *in situ* hybridization on the treated embryos with *krox20* (the molecular marker for r3 and r5) (29) and *myod* (the marker for somites) probes revealed

Table 1. Retention Time of Different Retinoids in Chromatographic Column

Source of Retinoids	Standard (min)	Vehicle (min)	Cyp26D1 (min)
All-trans RA	16.088	16.612	16.699
9-cis RA	15.740	15.955	16.069
13-cis RA	13.904	14.428	14.486
All-trans retinal	8.508		8.782
Retinol	8.785		8.385

Reverse-phase HPLC was performed using a Hypersil BDS C18 column. Listed are the retention times in the column of standard retinoids or unmetabolized retinoids after incubating with microsomes isolated from the cells transfected with vehicle vector or *cyp26d1* expression vector.

that the distance between r5 and s1 (Fig. 4, C and D; 0.88 ± 0.04 mm, $n = 33$; Table 3) was shorter than ($P < 0.01$) that of control embryos (Fig. 4, A and B; 1.28 ± 0.03 mm, $n = 33$; Table 3). We then microinjected zebrafish *cyp26a1* mRNA into zebrafish embryos, and the result showed that, like the DEAB-treated embryos (Fig. 4, C and D), the distance between r5 and s1 of the microinjected embryos (Fig. 4, E and F; 0.93 ± 0.29 mm, $n = 27$; Table 3) was also shorter than ($P < 0.01$) that of control embryos (Fig. 4, A and B; 1.28 ± 0.03 mm, $n = 33$; Table 3). When microinjecting *cyp26d1* mRNA into zebrafish embryos, we obtained the same result. The distance between r5 and s1 of the injected embryos (Fig. 4, G and H; 0.97 ± 0.23 , $n = 30$; Table 3) was also shorter than ($P < 0.01$) that of the control (Fig. 4, A and B; 1.28 ± 0.03 mm, $n = 33$; Table 3) but was approximately equal to ($P = 0.60$) that of embryos injected with *cyp26a1* (Fig. 4, E and F; 0.93 ± 0.29 , $n = 27$; Table 3). This result suggested that, like *cyp26a1*, zebrafish *cyp26d1* was involved in reducing RA activity *in vivo*.

Additionally, a recent report demonstrated that zebrafish *nls* embryos also have defects in left-right symmetry of somitogenesis during 6S–13S stages (13). Because *raldh2* is the major source for RA synthesis, we hypothesized that the embryos would have asymmetric somite development if their endogenous RA activities were reduced. To test this, we first examined $1 \mu\text{M}$ DEAB-treated embryos during 6S–13S stages. We found that 28 of 179 of treated embryos exhibited asymmetric somites, with 67.8% of them (19 of 28) having one to three extra somites on the right side (Fig. 5A and Table 4). The rate (15.6%; 28 of 179) of the treated embryos with asymmetric somites was significantly higher than ($P < 0.01$) that of control embryos (0 of 180), implying that reduction in endogenous RA activities results in asymmetric somitogenesis. We then microinjected zebrafish embryos with *cyp26a1*, the results showed that 33 of 132 embryos displayed asymmetric somites, with 60.6% (20 of 33) of those affected embryos having one to three extra somites on the left side (Fig. 5B and Table 4). The rate (25%; 33 of 132) of the *cyp26a1*-injected embryos with asymmetric somites was significantly higher than ($P < 0.01$) that

of control embryos (0 of 180). This is consistent with the role of *cyp26a1* in reducing RA activity *in vivo*. When microinjected with *cyp26d1*, 29 of 196 embryos showed asymmetric somites, of which 72.4% (21 of 29) had one to three extra somites on the right side (Fig. 5C and Table 3). The rate (14.8%; 29 of 196) of the *cyp26d1*-injected embryos with asymmetric somites was significantly higher than ($P < 0.01$) that of control embryos (0 of 180). The result further demonstrated that like *cyp26a1*, *cyp26d1* is also involved in reducing RA activity *in vivo*.

Tissue Distributions of the *cyp26d1* Gene

Previously, we have reported that *cyp26d1* has a unique dynamic expression pattern during early development of zebrafish (27). By performing RT-PCR analyses, we showed that zebrafish *cyp26d1* was also widely expressed in different adult tissues examined including brain, eye, heart, gill, liver, intestine, swimming bladder, ovary, muscle, caudal fin, and pectoral fin (Fig. 6A). However, the expression levels of *cyp26d1* in these tissues were different. Using Kodak ID Image Analysis software, we found that the relative expression levels in different tissues (calculated as the intensity of the amplified *cyp26d1* product divided by the intensity of amplified β -actin control product for each sample, and averaged over three independent experiments) were 0.028 ± 0.007 (brain), 0.050 ± 0.019 (caudal fin), 0.109 ± 0.021 (eye), 0.431 ± 0.101 (gill), 0.029 ± 0.002 (heart), 0.052 ± 0.013 (intestine), 0.023 ± 0.009 (liver), 0.309 ± 0.014 (muscle), 0.047 ± 0.019 (ovary), 0.124 ± 0.047 (pectoral fin), and 0.045 ± 0.017 (swimming bladder), respectively. Statistical tests showed that the abundance of *cyp26d1* message in different tissues were in this order: gill and muscle > eye and pectoral fin > brain, caudal fin, heart, intestine, liver, ovary, and swimming bladder (Fig. 6B).

DISCUSSION

Cyp26 family genes are known to encode enzymes that can specifically inactivate RA, and the first member, *cyp26a1*, was initially found in zebrafish (*cyp26a1*) (15). Until now, three different Cyp26 genes including *Cyp26A1*, *Cyp26B1*, and *Cyp26C1* have been identified in mammals. Of the three genes, orthologs of *Cyp26A1* and *Cyp26B1* genes have been found in zebrafish (15, 22). Previously, we cloned a novel *cyp26* gene in zebrafish and named it *cyp26d1* (27). While our results (AY920470) were in press (27), Kawakami et al. (13) published a paper reporting a zebrafish “Cyp26C1” sequence (AY904031). The authors used the “*cyp26c1*” as a probe for whole-mount *in situ* hybridization as part of the paper linking RA and left-right patterning without performing any functional analysis on it. However, analysis on this *cyp26c1*

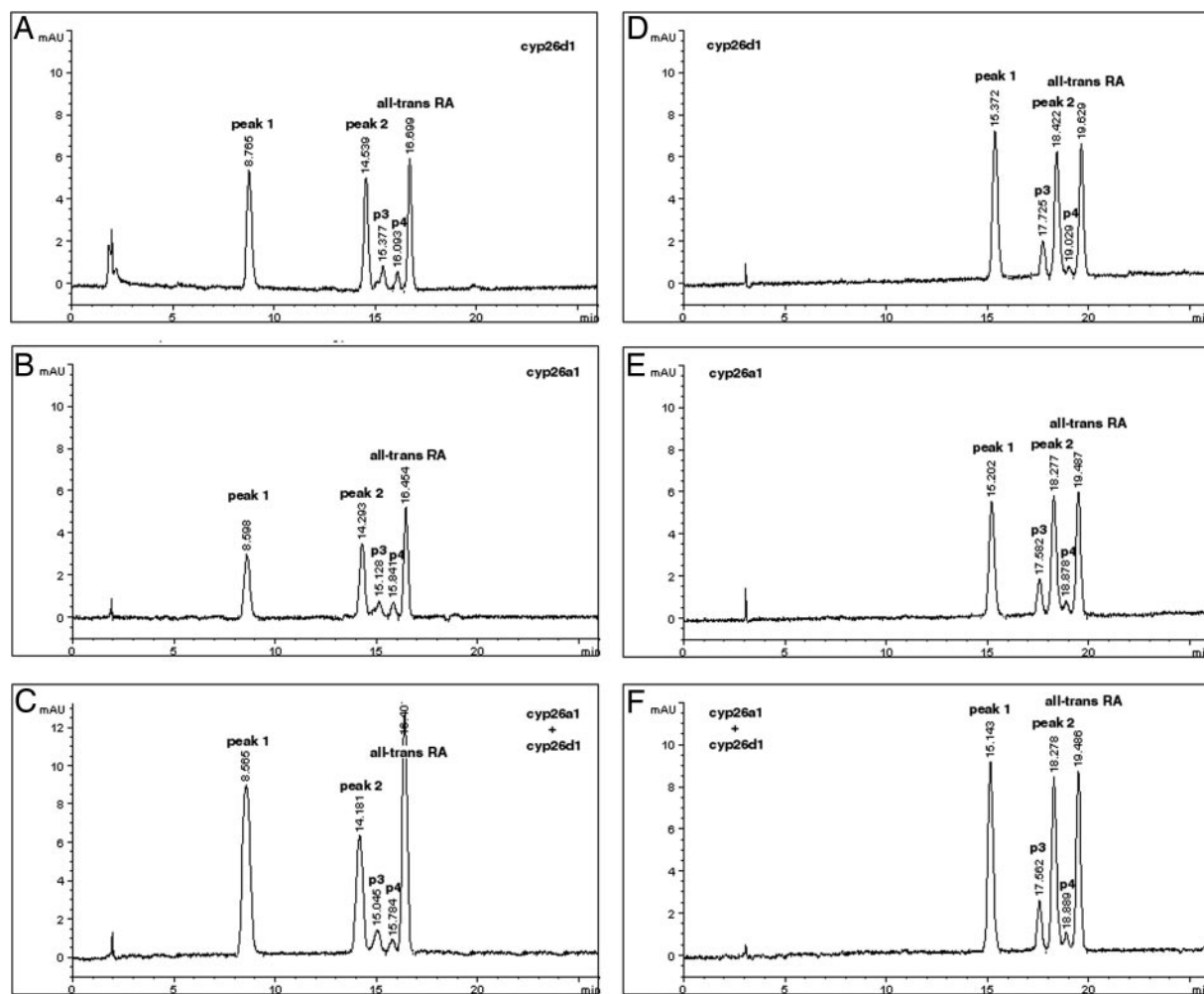


Fig. 3. HPLC Analysis Showing that Metabolites of All-trans RA Produced by Zebrafish Cyp26D1 Are Comigrating with Those Produced by Zebrafish Cyp26A1, Respectively

All-trans-RA was incubated with the microsomes isolated from 293T cells transfected with zebrafish *cyp26d1* and *cyp26a1*, respectively. By performing reverse-phase HPLC with Hypersil BDS C18 column (A and B) and SB-phenyl column (D and E), retinoids extracted from the reaction mixtures of Cyp26D1 (A and D) and Cyp26A1 (B and E) all displayed three major peaks plus two small peaks. Of the three major peaks in each chromatography, one peak had similar retention time to that of standard all-trans RA (Table 2) and therefore was recognized as the peak of unmetabolized substrate (as marked). When run by either Hypersil BDS C18 column (A and B) or SB-phenyl column (D and E), peak 1, peak 2, p3, and p4 from Cyp26D1 reaction mixture (A and D) had similar retention times to those from Cyp26A1 reaction mixture (B and E), respectively (Table 2). When the two sources of retinoids were mixed together, peak 1, peak 2, p3, p4, and the unmetabolized substrate were comigrating, respectively, either in Hypersil BDS C18 column (C) or in SB-phenyl column (F). Unmetabolized substrates were marked as judged by the retention time of standard all-trans RA (Table 2). x-axis, Retention time (in minutes) of retinoids; y-axis, absorbance value at 350 nm (mAU).

cDNA revealed that the AY904031 was an incomplete coding sequence without stop codon. When aligning AY904031 sequence with our *cyp26d1* cDNA, we found that it was only the 5'-part of our full-length coding cDNA. In our previous paper, we demonstrated that our cloned *cyp26d1* gene is not an ortholog of mammalian *Cyp26C1* genes (27). First, unlike zebrafish Cyp26A1 and Cyp26B1, which share more than 66 and 75% amino acid identities with their mammalian orthologs, respectively, zebrafish Cyp26D1 shares only 39–40% identity with mammalian Cyp26A1, 51% identity with mammalian Cyp26B1,

and 51–54% identity with mammalian Cyp26C1, respectively (27). This lower amino acid identity (<60%) suggests that zebrafish Cyp26D1 may define a new subfamily instead of being a member of the Cyp26C1 subfamily. Second, phylogenetic analyses revealed that evolutionarily this protein is closer to Cyp26B1 subfamily than to Cyp26C1 subfamily (27), which is consistent with the conclusion that this gene is not an ortholog of the mammalian *Cyp26C1* gene. Third, the physical locus of *Cyp26C1* is adjacent to *Cyp26A1* in chromosome 10q23 in humans (<http://www.ncbi.nlm.nih.gov>). The physical distance between the two genes

Table 2. Retention Time of RA Metabolites Produced by Cyp26A1 and Cyp26D1 in Chromatographic Columns

Source of Retinoids	Type of Columns							
	Hypersil BDS C18 Column				SB-Phenyl Column			
	Standard (min)	D1 (min)	A1 (min)	A1 + D1 (min)	Standard (min)	D1 (min)	A1 (min)	A1 + D1 (min)
All-trans-RA	16.088	16.699	16.454	16.402	19.340	19.629	19.487	19.486
Peak 1		8.765	8.598	8.565		15.372	15.202	15.143
Peak 2		14.539	14.293	14.181		18.422	18.277	18.278
p3		15.377	15.128	15.045		17.725	17.582	17.562
p4		16.093	15.841	15.784		19.029	18.878	18.889
9-cis-RA	15.740	16.069	15.962	15.430	19.213	19.154	19.111	18.928
Peak 1		8.714	8.637	8.043		15.441	15.375	15.195
13-cis-RA	13.904	14.486	14.262	14.163	18.377	18.275	18.223	18.496
Peak 1		8.778	8.374	8.543		15.157	15.088	15.379
Peak 2		16.577	16.447	16.390		19.479	19.424	19.718

Reverse-phase HPLC was performed using a Hypersil BDS C18 column and 20RBAX SB-Phenyl column. Listed are the retention times in the column of standard RA including all-trans-RA, 9-cis-RA, and 13-cis-RA, and the metabolites or unmetabolized substrates after RAs were incubated with microsomes isolated from the cells transfected with zebrafish *cyp26d1* expression vector (D1) or *cyp26a1* expression vector (A1), or the retinoids from the reaction mixtures of *cyp26d1* reaction and *cyp26a1* reaction (A1 + D1).

is 4778 bp long. However, *cyp26d1* is located in linkage group 17 (27) and *cyp26a1* is located in linkage group 12 in zebrafish (<http://zfin.org>). The facts further support the idea that *cyp26d1* is not an ortholog of the human *Cyp26C1* gene.

However, zebrafish Cyp26D1 contains all the predicted conserved functional domains in Cyp26s including anchor domain, praline-rich domain, oxygen binding domain, ligand binding domain, and heme-binding domain, implying that it is involved in RA metabolism. Through reverse HPLC analyses, we have demonstrated directly that, like other Cyp26 members (15–18, 20, 30), zebrafish Cyp26D1 specifically metabolized RA including the all-trans RA, 9-cis-RA, and 13-cis RA examined, but not retinol and retinal. The metabolites of all-trans RA produced by Cyp26D1 were found to be the same as that metabolized by zebrafish Cyp26A1, which are mainly 4-oxo-RA and 4-OH-RA (15). However, there are reports that suggested that the metabolites of all-trans RA produced by other Cyp26 members also include 18-OH-RA in addition to 4-oxo-RA and 4-OH-RA (16, 18, 20, 30) or 5,8-epoxy-RA (17). As suggested by Petkovich and coworkers (30), these discrepancies may arise from differences in metabolites extraction and characterization techniques. In this study, the HPLC analyses on metabolites of all-trans RA produced by Cyp26D1 and Cyp26A1 revealed that, in addition to the two major peaks (peak 1 and peak 2), there were two other small peaks (p3 and p4) present (Fig. 4), which is consistent with the idea that metabolites of all-trans RA metabolized by Cyp26s include four different retinoids.

A number of studies have shown that metabolites of all-trans RA including 4-oxo-RA, 4-OH-RA, 18-OH-RA, and 5,6-epoxy RA are all biologically active. For example, 4-oxo-RA was shown to be a highly active modulator in embryogenesis (31), and 4-oxo-RA, 4-OH-RA, and 5,6-epoxy-all-trans-RA (5,6-epoxy-RA)

could fully rescue the vitamin A-deficient quail embryo (32), while 4-oxo-, 4-OH-, 18-OH-, and 5,6-epoxy-RA could induce granulocytic differentiation of NB4 acute promyelocytic leukemia cells (33). Moreover, like all-trans RA, *in vitro* transcription assays had demonstrated that all four retinoids function through binding the RA response element of regulated genes (34). While using selective agonists against RAR, the metabolites were shown to regulate the Cyps through the RAR α receptor in quail embryos (32). However, when *Cyp26A1*^{-/-} homozygous mice were introduced into a *Raldh2*^{-/+} background, the *Cyp26A1*-null phenotypes were suppressed. The *Cyp26A1*^{-/-}/*Raldh2*^{-/+} mouse could survive to adulthood without any phenotypic defect apart from their abnormal tails, and both males and females of the surviving *Cyp26A1*^{-/-}/*Raldh2*^{-/+} mice were fertile (6). These findings provide direct genetic evidence that the normal function of Cyp26A1 is opposite to that of *Raldh2*, and Cyp26A1 may play a role in preventing inappropriate RA signaling, rather than producing signaling by bioactive RA metabolites such as 4-oxo-RA, 4-OH-RA, and 5,6-epoxy-RA. These data are consistent with the fact that overexpression of *Cyp26A1* in *Xenopus laevis* embryos can rescue the developmental defects induced by exogenous excess RA (35). In zebrafish, *nls* embryos with *raldh2* mutation were characterized by a truncation of the anteroposterior axis anterior to the somites (11), whereas *giraffe* embryos with *cyp26a1* mutation had an expanded rostral spinal cord territory (26). The opposite phenotypes of *nls* embryos and *giraffe* embryos again suggested that *raldh* and *cyp26* work together to establish local embryonic RA levels that must be finely tuned to allow normal development of embryos. For example, the development of the anteroposterior axis anterior to the somites seemed to largely depend on the endogenous RA activity. And the length of anteroposterior axis appeared to corre-

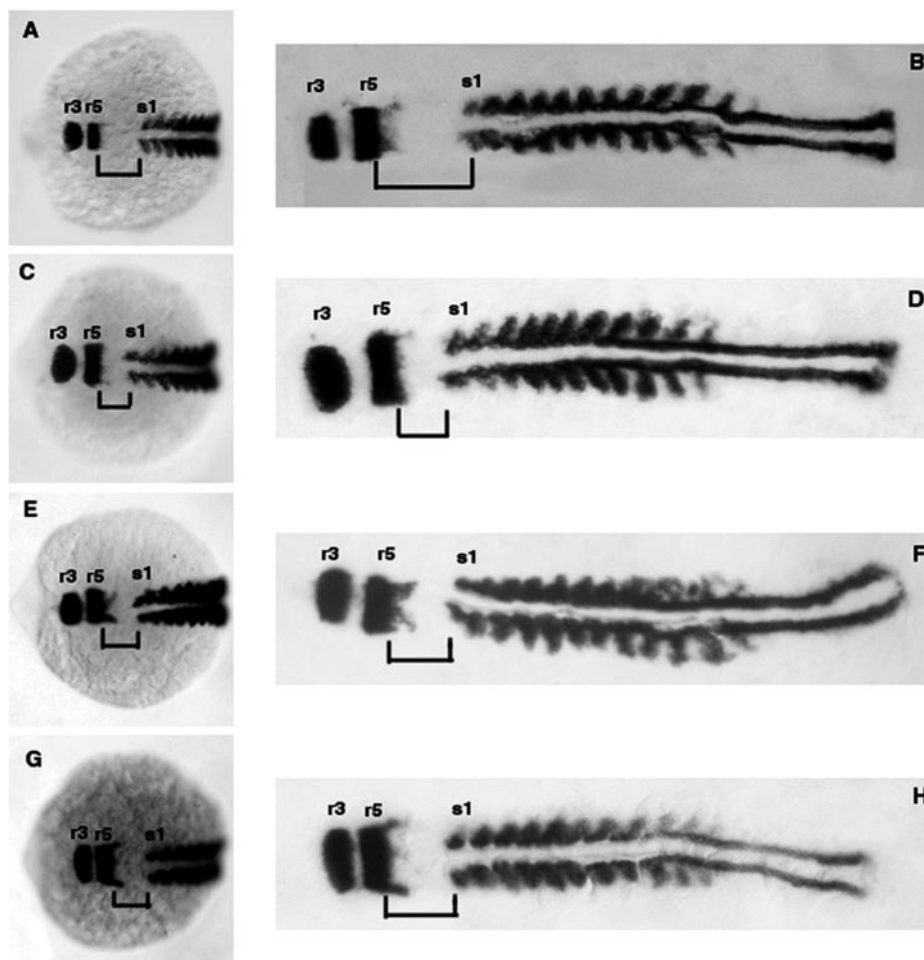


Fig. 4. *In Vivo* Assay Showing that Overexpression of Cyp26D1 in Zebrafish Embryos Can Shorten the Anterior-Posterior Axes of the Embryos

Embryos (11-somite stage) were whole-mount *in situ* hybridized with *krox20* and *myod* probes. A, C, E, and G, Dorsal view. *Left*, Anterior; *right*, posterior. B, D, F, and H, Flat mount of embryos, dorsal view. *Left*, Anterior; *right*, posterior. A and B, Control embryos with mock injection. C and D, Embryos treated with 1 μ M DEAB. E and F, Embryos microinjected with *cyp26a1* mRNA. G and H, Embryos microinjected with *cyp26d1*. The distance between r5 and s1 (marked) of 1 μ M DEAB-treated (C and D), *cyp26a1* mRNA-microinjected (E and F), and *cyp26d1*-microinjected (G and H) embryos is shorter than that of control embryos with mock injection (A and B).

late positively with the amount of RA activity, that is, lower RA activity would result in a shorter axis and higher RA activity would result in a longer axis. By treating embryos with DEAB, which can specifically inhibit endogenous RA synthesis (36), we revealed

that, like *nls* embryos, the DEAB-treated embryos had a short “neck,” that is, the distance between r5 and s1 was shorter than that of untreated embryos. Based on this observation, we next examined the *in vivo* activity of *cyp26d1* by microinjecting embryos with *cyp26d1*

Table 3. Distances between r5 and the s1 of 11S Zebrafish Embryos after Different Treatments

Treatment	Control (mm)	1 μ M DEAB (mm)	Cyp26A1 (mm)	Cyp26D1 (mm)
Experiment 1	1.29 \pm 0.02 (n = 11)	0.89 \pm 0.03 (n = 11)	0.94 \pm 0.39 (n = 8)	1.01 \pm 0.20 (n = 14)
Experiment 2	1.28 \pm 0.03 (n = 11)	0.88 \pm 0.05 (n = 11)	1.04 \pm 0.22 (n = 8)	0.95 \pm 0.27 (n = 8)
Experiment 3	1.27 \pm 0.04 (n = 11)	0.87 \pm 0.03 (n = 11)	0.85 \pm 0.26 (n = 11)	0.91 \pm 0.27 (n = 8)
Total	1.28 \pm 0.03 (n = 33)	0.88 \pm 0.04 (n = 33)	0.93 \pm 0.29 (n = 27)	0.97 \pm 0.23 (n = 30)

The distances between r5 and s1 of 11S were measured on the whole-mount embryos that were *in situ* hybridized with *krox20* (the molecular marker for r3 and r5) and *myod* (the marker for somites). The distance is shown as the average value \pm SD in millimeters. n is the number of the embryos measured.

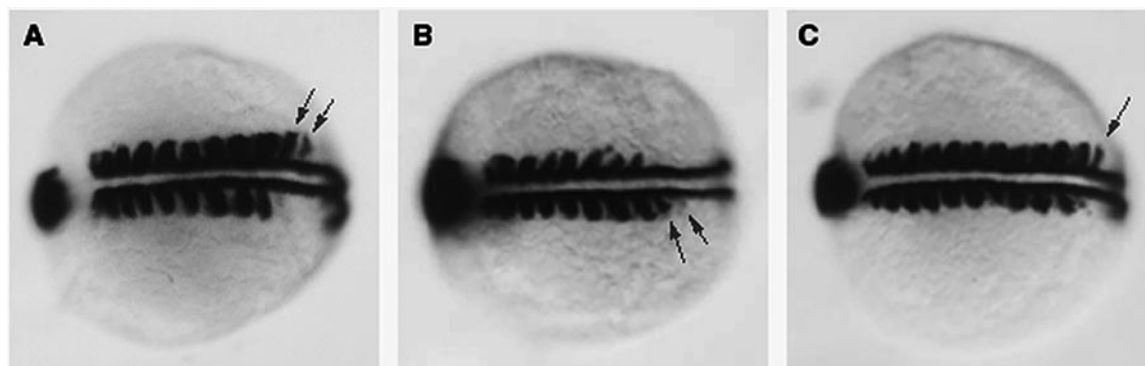


Fig. 5. *In Vivo* Assay Showing that Overexpression of Cyp26D1 in Zebrafish Embryos Can Cause Asymmetric Somite Formation of the Embryos

Embryos were treated at the one- to four-cell stage and allowed to develop to six- to 13-somite stages. Embryos were then fixed, and whole-mount *in situ* hybridization with *krox20* and *myod* probes was performed. Embryos were positioned *dorsal* forward, *left* anterior, and *right* posterior. A, Embryos incubated with 1 μM DEAB; 11-somite stage. B, Embryo microinjected with *cyp26a1* mRNA; 10-somite stage. C, Embryos microinjected with *cyp26d1* mRNA; 13-somite stage. Arrows indicate extra somites.

mRNA, and then measured the distance between r5 and s1. We showed that overexpression of *cyp26d1* genes in embryos caused a shortened distance between r5 and s1, similar to the *cyp26a1* overexpression phenotype in zebrafish embryos and to the phe-

notype of the DEAB-treated embryos. This result is consistent with our hypothesis that the *in vivo* role of *cyp26d1* is to reduce RA activity and the metabolites of all-trans RA produced by Cyp26D1 are biologically inactive. Moreover, recent discoveries have revealed that blocking endogenous RA activities can disrupt the bilateral symmetry of somite formation in vertebrates (9, 10, 13). We demonstrated that treating embryos with 1 μM DEAB disrupted the left-right symmetry in somite development. Because 1 μM DEAB can only partly inhibit endogenous RA synthesis (36), the result suggested that partial reduction of endogenous RA activity can also cause asymmetric somite development. We also observed this somite asymmetry phenotype in zebrafish embryos microinjected with *cyp26a1* or *cyp26d1* mRNA. Together, our study provided *in vivo* evidence that *cyp26d1* gene is responsible for the degradation of RA.

Previously, we have described that *cyp26d1* has a dynamic expression during the early development of zebrafish (27). Here, we found that *cyp26d1* is also widely expressed in adults but with different individual expression levels, suggesting that *cyp26d1* could play important roles not only in embryogenesis but also in the growth of adult organs.

MATERIALS AND METHODS

Experimental Animals

Research on the zebrafish used in this study was conducted in accordance with accepted standards of humane animal care.

Detection of *cyp26d1* Expression in Adult Zebrafish Organs

The distributions of *cyp26d1* in adult organs were detected by RT-PCR method. Different organs from adult zebrafish

Table 4. Asymmetric Somite Development of Zebrafish Embryos after Incubation with DEAB or Microinjection with Zebrafish *cyp26a1* and *cyp26d1* mRNA

	Number of Embryos		Asymmetric Somites	
	Total	Asymmetric Embryos	Left-Sided	Right-Sided
Control				
Experiment 1	60	0	0	0
Experiment 2	60	0	0	0
Experiment 3	60	0	0	0
Subtotal	180	0	0	0
1 μM DEAB				
Experiment 1	59	9	2	7
Experiment 2	60	10	2	8
Experiment 3	60	9	5	4
Subtotal	179	28	9	19
<i>cyp26a1</i> injected				
Experiment 1	27	7	5	2
Experiment 2	40	10	7	3
Experiment 3	65	16	8	8
Subtotal	132	33	20	13
<i>cyp26d1</i> injected				
Experiment 1	22	3	0	3
Experiment 2	60	13	5	8
Experiment 3	114	13	3	10
Subtotal	196	29	8	21

Zebrafish embryos incubated with 1 μM DEAB or injected with zebrafish *cyp26a1* and *cyp26d1* mRNA or mock injection control, respectively, at the one- to four-cell stage were allowed to develop and fixed between 6- and 13-somite stages. The somitogenesis was scored by means of *myod* whole-mount *in situ* hybridization.

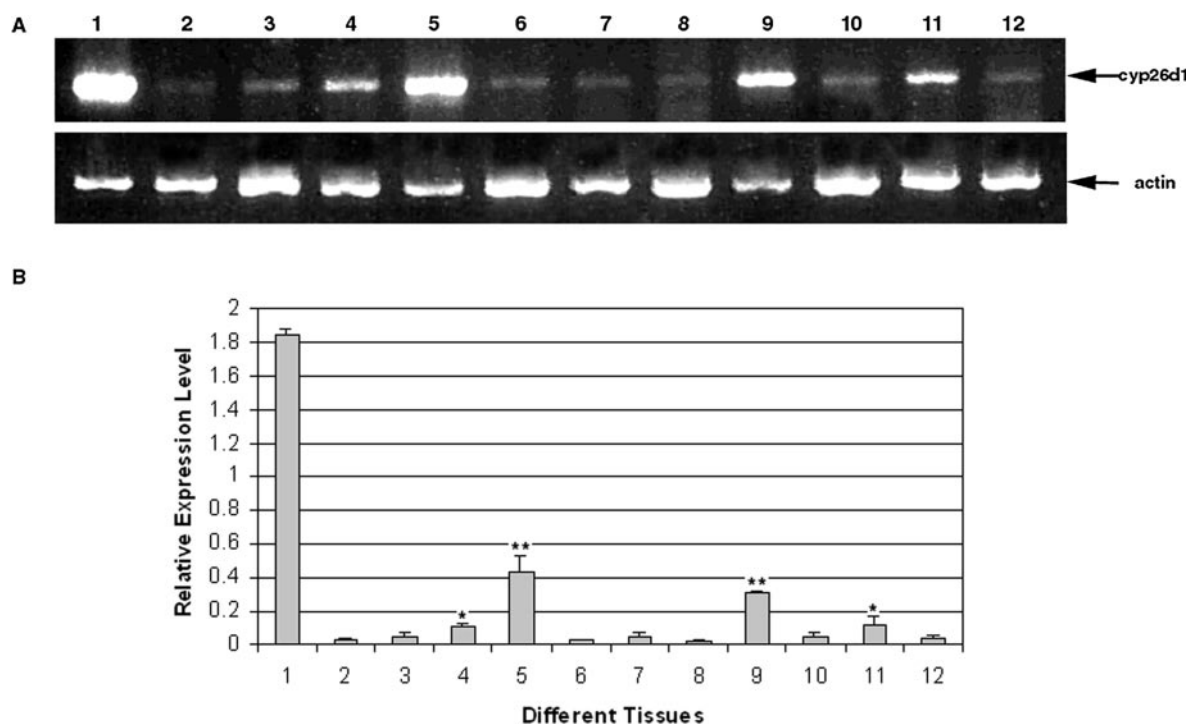


Fig. 6. RT-PCR Analysis Showing Expression Pattern of *Cyp26d1* Gene in Different Adult Organs

A, Amplified products were separated in 0.8% agarose gel, stained with ethidium bromide, and photographed by Kodak EDAS 290. An 837-bp fragment of *cyp26d1* cDNA was detected from different adult organs. Expression of zebrafish β -actin was detected as a control of RT-PCR sensitivity using same RNA template as above. B, The expression levels of *cyp26d1* varied in different adult organs. Data were normalized by dividing the intensity of amplified *cyp26d1* product by the intensity of amplified β -actin control product for each sample. The intensity of the amplified product was measured using Kodak ID Image Analysis software. Results were subjected to Student's *t* test. **, The expression levels of *cyp26d1* in gill and muscle are much higher than ($P < 0.01$) that in other organs. *, The expression levels of *cyp26d1* in eye and pectoral fin are significantly higher than ($P < 0.05$) that in brain, caudal fin, heart, intestine, liver, ovary, and swimming bladder. Lane 1, *cyp26d1* cDNA template as positive control; 2, brain; 3, caudal fin; 4, eye; 5, gill; 6, heart; 7, intestine; 8, liver; 9, muscle; 10, ovary; 11, pectoral fin; 12, swimming bladder.

were collected to extract total RNA using Trizol reagent (Invitrogen, Carlsbad, CA) following the manufacturer's protocol. Reverse transcription of RNA was carried out with Moloney murine leukemia virus reverse transcriptase (Promega, Madison, WI). The sequences of primers used to detect presence of *cyp26d1* cDNA were 5'-AAGTCACTCACCTTC-CGC-3' (forward) and 5'-GAAACGGTCTGGGTCAAA-3' (reverse). PCR was performed using Taq DNA polymerase (Promega) and the conditions were 94 C for 2 min; 40 cycles of 94 C, 30 sec; 54 C, 45 sec; 72 C, 1 min; followed by 10-min incubation at 72 C. The sensitivity of the RT-PCR was controlled by performing the amplification (20 cycles) of zebrafish β -actin using the same cDNA templates as described before (37). The amplified products were run in 0.8% native agarose gel, stained with ethidium bromide, and photographed by Kodak Electrophoresis Documentation and Analysis System (EDAS) 290. The intensities of amplified products were measured using Kodak ID Image Analysis software on the ethidium bromide-stained gel. The relative expression levels were normalized by dividing the intensity of amplified *cyp26d1* product by the intensity of amplified β -actin control product. The experiment was repeated three times independently. The data were subjected to Student's *t* test.

Expression of Zebrafish *cyp26d1* and *cyp26a1* Genes in 293T Cells by Transient Transfection

To express zebrafish *cyp26d1* and *cyp26a1* genes, we first cloned *cyp26d1* and *cyp26a1* coding sequences (GenBank

nos. AY920470 and U68234). Expression vectors of the genes were constructed by recombining the coding sequences with a preceding Kozak sequence into pcDNA3.1 (Invitrogen). The inserts were sequenced to confirm their identities. Transient transfections of 293T cells (American Type Culture Collection, Manassas, VA) with the expression vectors or vehicle vector pcDNA3.1 were performed using Lipofectamine (Invitrogen) following the manufacturer's manuals. Cells were harvested 48 h after transfection and microsome fractions were prepared from the cultured cells by centrifugation at $100,000 \times g$ after the cells were sonicated.

In Vitro RA-Metabolizing Assay

The *in vitro* RA-metabolizing activities of Cyp26s were analyzed according to the method described previously (17). Briefly, the standard reaction mixture in 1 ml contains microsome fractions (from five 100-mm dishes) in a reaction buffer [10 mM NADP, 0.1 M glucose-6-phosphate, 50 mM K_2HPO_4 (pH 7.5), 0.2 mM $MgCl_2$, 1 U glucose-6-phosphate dehydrogenase] [chemicals were bought from Sigma (St. Louis, MO)]. After adding 1 μ g of each retinoid dissolved in 3 μ l of dimethylsulfoxide to the reaction, the mixture was incubated in a light-protected tube at 37 C for 2 h. The metabolites plus unmetabolized substrate from the reaction mixture were then extracted, concentrated, and analyzed as described previously (38). The resulting residues were dissolved in 80 μ l of 2-propanol for reverse-phase HPLC analysis.

Reverse-Phase HPLC Analysis on Retinoids

The retinoids were detected by reverse-phase HPLC at a wavelength of 350 nm and at 35 °C of the column temperature with HP 1050 HPLC instrument (Hewlett Packard, Palo Alto, CA). Two different types of columns were used to separate retinoids. One of the columns is Hypersil BDS C18 (150 × 4.6 mm, 5 μm; Dalian Elite, Dalian, China). The solution and program of elution used in this column were described previously (17, 38). Briefly, the mobile phase consisted of two solvents (solvent A, methanol-acetonitrile, 8:2 (vol/vol); solvent B, 2% acetic acid). The flow rate of the elution was 1.0 ml/min. And the gradient program was followed as such: 80:20 of solvent A to solvent B (vol/vol) was used to elute for first 8 min, followed by a second 8-min linear gradient up to 90:10 (vol/vol), then at the fixed ratio eluted for the third 8 min, and finally returned to 80:20 (vol/vol) and eluted for the last 2 min. A second column was 20RBAX SB-phenyl (250 × 4.6 mm, 5 μm; Agilent Technologies, Kista, Sweden). The components of the mobile phase for eluting this column and the elution rate were the same as used in C18 column. However, the gradient program was changed such that 72:28 of solvent A to solvent B (vol/vol) was first used to elute for the first 10 min, followed by a second 10-min linear gradient up to 81:19 (vol/vol), and then at the fixed ratio eluted for another 4 min, and finally returned to 72:28 (vol/vol) and eluted for the last 2 min.

In Vivo RA-Metabolizing Assay

To test Cyp26D1 activities *in vivo*, mRNAs of *cyp26d1* and *cyp26a1* were synthesized *in vitro*. Briefly, full-length cDNA sequences of *cyp26d1* (AY920470) and *cyp26a1* (U68234) were introduced into pBluescript vector (Stratagene, La Jolla, CA) under T7 promoter direction. mRNAs of *cyp26d1* and *cyp26a1* were synthesized and capped *in vitro* using mMES-SAGE mMACHINE T7 Ultra kit (Ambion, Austin, TX). About 2–3 nl of 0.5 μg/μl mRNAs were injected into zebrafish embryos at the one- to four-cell stage. In the meantime, embryos treated with 1 μM DEAB (an inhibitor of Raldhs; Sigma) at the one-cell stage served as positive controls, and the embryos injected with the same amount of nanopure water (mock injection) served as negative controls. All of the embryos were then allowed to grow at 28.5 °C and fixed at about 11-somite stages to do double whole-mount *in situ* hybridization to detect the expressions of *krox20* in hindbrain and *myod* in somites. Whole-mount *in situ* hybridization was performed as described previously (22). Both probes were labeled with 11-Dig-UTP (Roche, Basel, Switzerland). During hybridization, the two probes were added together and the concentrations of the RNA probes used in hybridization were 0.5 ng/μl. After whole-mount *in situ* hybridization, the distances between r5 and s1 of 11S embryos were measured and the number of embryos during 6S–13S stages with asymmetric somites was recorded. The experiment was repeated three times independently. The data were subjected to Student's *t* test (for distances between r5 and s1) or χ^2 test (for asymmetric somitogenesis). Images were captured using a digital camera.

Acknowledgments

We thank Dr. Anming Meng for kindly providing us with the RNA probe template of zebrafish *myod* gene; Hongzhao Li, Zhijing He, and Li Liu for their technical assistance in cell sonication, ultracentrifuge, and HPLC during the course of this work; and Dr. Jiong Chen for his help in editing the manuscript.

Address all correspondence and requests for reprints to: Dr. Qingshun Zhao, Model Animal Research Center, Nanjing University, 12 Xuefu Road, Pukou District, Nanjing 210061, China. E-mail: qingshun@nicemice.cn.

This work was supported by China "973 Project" (2005CB522501) (to X.Ga.) and grants from the National Natural Science Foundation of China (30370722) and the Scientific Research Foundation for the Returned Overseas Chinese Scholars (State Education Ministry, China) (to Q.Z.).

X.Gu, F.X., W.S., X.W., P.H., Y.Y., X.Ga., and Q.Z. have nothing to declare.

REFERENCES

1. Kalter H, Warkany J 1959 Experimental production of congenital malformations in mammals by metabolic procedure. *Physiol Rev* 39:69–115
2. Shenefelt RE 1972 Morphogenesis of malformations in hamsters caused by retinoic acid: relation to dose and stage at treatment. *Teratology* 5:103–118
3. Chambon P 1996 A decade of molecular biology of retinoic acid receptors. *FASEB J* 10:940–954
4. Mark M, Ghyselinck NB, Wendling O, Dupé V, Mascres B, Kastner P, Chambon P 1999 A genetic dissection of the retinoid signalling pathway in the mouse. *Proc Nutr Soc* 3:609–613
5. Ross SA, McCaffery PJ, Drager UC, De Luca LM 2000 Retinoids in embryonal development. *Physiol Rev* 80: 1021–1054
6. Niederreither K, Abu-Abed S, Schuhbauer B, Petkovich M, Chambon P, Dolle P 2002 Genetic evidence that oxidative derivatives of retinoic acid are not involved in retinoid signaling during mouse development. *Nat Genet* 31: 84–88
7. Fan X, Molotkov A, Manabe S, Donmoyer CM, Deltour L, Foglio MH, Cuenca AE, Blaser WS, Lipton SA, Duester G 2003 Targeted disruption of *Aldh1a1* (*Raldh1*) provides evidence for a complex mechanism of retinoic acid synthesis in the developing retina. *Mol Cell Biol* 23: 4637–4648
8. Niederreither K, Subbarayan V, Dolle P, Chambon P 1999 Embryonic retinoic acid synthesis is essential for early mouse post-implantation development. *Nat Genet* 21: 444–448
9. Vermot J, Gallego LJ, Fraulob V, Niederreither K, Chambon P, Dolle P 2005 Retinoic acid controls the bilateral symmetry of somite formation in the mouse embryo. *Science* 308:563–566
10. Vermot J, Pourquie O 2005 Retinoic acid coordinates somitogenesis and left-right patterning in vertebrate embryos. *Nature* 435:215–220
11. Begemann G, Schilling TF, Rauch GJ, Geisler R, Ingham PW 2001 The zebrafish neckless mutation reveals a requirement for *raldh2* in mesodermal signals that pattern the hindbrain. *Development* 128:3081–3094
12. Grandel H, Lun K, Rauch GJ, Rhinn M, Piotrowski T, Houart C, Sordino P, Kuchler AM, Schulte-Merker S, Geisler R, Holder N, Wilson SW, Brand M 2002 Retinoic acid signalling in the zebrafish embryo is necessary during pre-segmentation stages to pattern the anterior-posterior axis of the CNS and to induce a pectoral fin bud. *Development* 129:2851–2865
13. Kawakami Y, Raya A, Raya RM, Rodriguez-Esteban C, Belmonte JC 2005 Retinoic acid signalling links left-right asymmetric patterning and bilaterally symmetric somitogenesis in the zebrafish embryo. *Nature* 435:165–171
14. Dupe V, Matt N, Garnier JM, Chambon P, Mark M, Ghyselinck NB 2003 A newborn lethal defect due to inactivation of retinaldehyde dehydrogenase type 3 is prevented by maternal retinoic acid treatment. *Proc Natl Acad Sci USA* 100:14036–14041

Received September 7, 2005. Accepted January 24, 2006.

15. White JA, Guo YD, Baetz K, Beckett-Jones B, Bonasoro J, Hsu KE, Dilworth FJ, Jones G, Petkovich M 1996 Identification of the retinoic acid-inducible all-*trans*-retinoic acid 4-hydroxylase. *J Biol Chem* 271:29922–29927
16. White JA, Beckett-Jones B, Guo Y-D, Dilworth FJ, Bonasoro J, Jones G, Petkovich M 1997 cDNA cloning of human retinoic acid-metabolizing enzyme (hP450RAI) identifies a novel family of cytochromes P450 (CYP26). *J Biol Chem* 272:18538–18541
17. Fujii H, Sato T, Kanekol S, Gotoh O, Fujii-Kuriyama Y, Osawa K, Kato S, Hamada H 1997 Metabolic inactivation of retinoic acid by a novel P450 differentially expressed in developing mouse embryos. *EMBO J* 16:4163–4173
18. White JA, Ramshaw H, Taimi M, Stangle W, Zhang A, Everingham S 2000 Identification of the human cytochrome P450, P450RAI-2, which is predominantly expressed in the adult cerebellum and is responsible for all-*trans*-retinoic acid metabolism. *Proc Natl Acad Sci USA* 97:6403–6408
19. MacLean G, Abu-Abed S, Dolle P, Tahayato A, Chambon P, Petkovich M 2001 Cloning of a novel retinoic-acid metabolizing cytochrome P450 Cyp26B1, and comparative expression analysis with Cyp26A1 during early murine development. *Mech Dev* 107:195–201
20. Taimi M, Helvig C, Wisniewski J, Ramshaw H, White J, Amad M, Korczak B, Petkovich M 2004 A novel human cytochrome P450, CYP26C1, involved in metabolism of 9-*cis* and all-*trans* isomers of retinoic acid. *J Biol Chem* 279:77–85
21. Tahayato A, Dolle P, Petkovich M 2003 Cyp26C1 encodes a novel retinoic acid-metabolizing enzyme expressed in the hindbrain, inner ear, first branchial arch and tooth buds during murine development. *Gene Expr Patterns* 3:449–454
22. Zhao Q, Dobbs-McAuliffe B, Linney E 2005 Expression of cyp26b1 during zebrafish early development. *Gene Expr Patterns* 5:363–369
23. Abu-Abed S, Dolle P, Metzger D, Beckett B, Chambon P, Petkovich M 2001 The retinoic acid-metabolizing enzyme, CYP26A1, is essential for normal hindbrain patterning, vertebral identity, and development of posterior structures. *Genes Dev* 15:226–240
24. Sakai Y, Meno C, Fujii H, Nishino J, Shiratori H, Saijoh Y, Rossant J, Hamada H 2001 The retinoic acid-inactivating enzyme CYP26 is essential for establishing an uneven distribution of retinoic acid along the antero-posterior axis within the mouse embryo. *Genes Dev* 15:213–225
25. Yashiro K, Zhao X, Uehara M, Yamashita K, Nishijima M, Nishino J, Saijoh Y, Sakai Y, Hamada H 2004 Regulation of retinoic acid distribution is required for proximodistal patterning and outgrowth of the developing mouse limb. *Dev Cell* 6:411–422
26. Emoto Y, Wadab H, Okamoto H, Kudo A, Imaia Y 2005 Retinoic acid-metabolizing enzyme Cyp26a1 is essential for determining territories of hindbrain and spinal cord in zebrafish. *Dev Biol* 278:415–427
27. Gu X, Xu F, Wang X, Gao X, Zhao Q 2005 Molecular cloning and expression of a novel CYP26 gene (cyp26d1) during zebrafish early development. *Gene Expr Patterns* 5:733–739
28. Ray WJ, Bain G, Yao M, Gottlieb DI 1997 CYP26, a novel mammalian cytochrome P450, is induced by retinoic acid and defines a new family. *J Biol Chem* 272:18702–18708
29. Oxtoby E, Jowett T 1993 Cloning of the zebrafish krox-20 gene (krx-20) and its expression during hindbrain development. *Nucleic Acids Res* 21:1087–1095
30. Abu-Abed SS, Beckett BR, Chiba H, Chithalani JV, Jones G, Metzger D, Chambon P, Petkovich M 1998 Mouse P450RAI (CYP26) expression and retinoic acid-inducible retinoic acid metabolism in F9 cells are regulated by retinoic acid receptor γ and retinoid X receptor α . *J Biol Chem* 273:2409–2415
31. Pijnappel WW, Hendriks HF, Folkers GE, van den Brink CE, Dekker EJ, Edelenbosch C, van der Saag PT, Durston AJ 1993 The retinoid ligand 4-oxo-retinoic acid is a highly active modulator of positional specification. *Nature* 366:340–344
32. Reijntjes S, Blentic A, Gale E, Maden M 2005 The control of morphogen signalling: regulation of the synthesis and catabolism of retinoic acid in the developing embryo. *Dev Biol* 285:224–237
33. Idres N, Benoit G, Flexor MA, Lanotte M, Chabot GG 2001 Granulocytic differentiation of human NB4 promyelocytic leukemia cells induced by all-*trans* retinoic acid metabolites. *Cancer Res* 61:700–705
34. Idres N, Marill J, Flexor MA, Chabot GG 2002 Activation of retinoic acid receptor-dependent transcription by all-*trans*-retinoic acid metabolites and isomers. *J Biol Chem* 277:31491–31498
35. Hollemann T, Chen Y, Grunz H, Pieler T 1998 Regionalized metabolic activity establishes boundaries of retinoic acid signalling. *EMBO J* 17:7361–7372
36. Perz-Edwards A, Hardison NL, Linney E 2001 Retinoic acid-mediated gene expression in transgenic reporter zebrafish. *Dev Biol* 229:89–101
37. Sun L, Zou Z, Collodi P, Xu F, Xu X, Zhao Q 2005 Identification and characterization of a second fibronectin gene in zebrafish. *Matrix Biol* 24:69–77
38. Kojima R, Fyjmori T, Kiyota N, Toriya Y, Fukuda T, Ohashi T, Sato T, Yoshizawa Y, Takeyama K, Mano H, Masushige S, Kato S 1994 *In vivo* isomerization of retinoic acids. Rapid isomer exchange and gene expression. *J Biol Chem* 269:32700–32707

